

INFLORESCENCE DEFICIENT IN ABSCISSION Controls Floral Organ Abscission in Arabidopsis and Identifies a Novel Family of Putative Ligands in Plants

Melinka A. Butenko,^a Sara E. Patterson,^b Paul E. Grini,^a Grethe-Elisabeth Stenvik,^a Silja S. Amundsen,^{a,1} Abul Mandal,^c and Reidunn B. Aalen^{a,2}

^aDivision of Cell and Molecular Biology, University of Oslo, N-0315 Oslo, Norway

^bDepartment of Horticulture, University of Wisconsin-Madison, Madison, Wisconsin 53706-1381

^cDepartment of Natural Sciences, University of Skövde, 54128 Skövde, Sweden

Abscission is an active process that enables plants to shed unwanted organs. Because the purpose of the flower is to facilitate pollination, it often is abscised after fertilization. We have identified an Arabidopsis ethylene-sensitive mutant, *inflorescence deficient in abscission (ida)*, in which floral organs remain attached to the plant body after the shedding of mature seeds, even though a floral abscission zone develops. The *IDA* gene, positioned in the genomic DNA flanking the single T-DNA present in the *ida* line, was identified by complementation. The gene encodes a small protein with an N-terminal signal peptide, suggesting that the *IDA* protein is the ligand of an unknown receptor involved in the developmental control of floral abscission. We have identified Arabidopsis genes, and cDNAs from a variety of plant species, that encode similar proteins, which are distinct from known ligands. *IDA* and the *IDA*-like proteins may represent a new class of ligands in plants.

INTRODUCTION

Abscission, a physiologically determined program of cell separation, provides a mechanism whereby every discrete, multicellular plant organ, such as leaves, flowers, or fruits, becomes detached from the plant body in a controlled manner (Sexton and Roberts, 1982). Abscission can be initiated in response to environmental events such as disease or pathogens, or it can be a programmed shedding of organs that no longer provide essential function to the plant, exemplified by the flower after aiding in pollination (Bleecker and Patterson, 1997). The process requires the formation of an anatomically distinct structure, the abscission zone (AZ), which constitutes the region where organs are detached from the plant body (Addicott, 1982). Very little is known about which developmental signals and how cell–cell interactions inform primordial AZ cells to differentiate (González-Carranza et al., 2002).

Arabidopsis does not display leaf or fruit abscission, but it is an interesting model for floral abscission because it sheds intact turgid floral organs (Patterson, 2001). Thus, the Arabidopsis abscission process is not obscured by phenomena associated with senescence. The cells of the floral organ AZ (consisting of filament, petal, and sepal) of Arabidopsis are determined by the presence of small and densely cytoplasmic cells (Bleecker and Patterson, 1997). Soon after anthesis, the separation of floral organs takes place as an active form of programmed abscission (Patterson et al., 1994; Bleecker and Patterson, 1997). The pro-

cess can be divided into several steps (Patterson, 2001). After the AZ has formed at the junction between the flower receptacle and floral organs, this zone acquires the competence to respond to abscission signals, and the cell separation process commences. This is accompanied by the elongation of cells at the plant body side of the AZ. It is not clear whether this elongation is a necessary step in the abscission process or a result of this process. The middle lamella between the cells in the AZ is degraded by enzymatic hydrolysis, and at the plant body side of the AZ a protective layer differentiates.

Evidence from many different abscission model systems supports ethylene's promotional and auxin's inhibitory role in the regulation of abscission in dicotyledonous plants (Abeles, 1968; Addicott, 1982; Roberts et al., 1984; Woltering and Van Doorn, 1988; Brown, 1997; Van Doorn and Stead, 1997). However, it is doubtful whether ethylene also is the sole inducer and regulator of the gene expression program that causes separation (González-Carranza et al., 1998).

Recent reports indicate a subordinate role for ethylene in floral organ abscission in Arabidopsis, by showing that reduction of the protein level of the Leu-rich repeat (LRR) receptor-like kinase (RLK) HAESA delays floral abscission (Jinn et al., 2000) and that overexpression of the MADS domain factor AGL15 results in delayed abscission (Fernandez et al., 2000), although the ethylene responses of these plants were normal. The ethylene-insensitive Arabidopsis mutants *etr1* (Bleecker et al., 1988) and *ein2* (Guzman and Ecker, 1990) also show a considerable delay in floral abscission, but comparative studies demonstrate that these mutants go through virtually the same developmental progression as wild-type plants (Patterson et al., 1994; Bleecker and Patterson, 1997). Thus, during floral organ abscission in Arabidopsis, the assumed essential role of ethylene may be a misconception, and it is conceivable that developmental pathways indepen-

¹Current address: Department of Immunology, Rikshospitalet, Sogns-vannsveien 20, 0027 Oslo, Norway.

²To whom correspondence should be addressed. E-mail reidunn.aalen@bio.uio.no; fax 47-22854605.

Article, publication date, and citation information can be found at www.plantcell.org/cgi/doi/10.1105/tpc.014365.

dent of ethylene may regulate floral organ abscission (Bleecker and Patterson, 1997).

Here, we present an *Arabidopsis* mutant, *inflorescence deficient in abscission* (*ida*), that retains its floral organs indefinitely. This deficiency is not influenced by ethylene, although *ida* otherwise shows normal ethylene sensitivity. A comparative analysis of floral organ abscission between wild-type and *ida* mutant plants, as well as in the *etr1-1* mutant, suggests that the mutation mainly affects the last step(s) of the abscission process. *IDA* encodes a novel protein with properties that suggest that it is a ligand. Bioinformatics was used to identify cDNAs and genes that encode similar proteins in a number of plant species.

RESULTS

The Mutant *ida* Develops an AZ but Is Deficient in Floral Abscission

In screening for mutants delayed in floral abscission, we identified the *ida* mutant in a collection of *Arabidopsis* lines transformed with the T-DNA vector pMHA2 (Mandal et al., 1995). In wild-type *Arabidopsis* flowers, the shedding of turgid flower petals, sepals, and stamens supervened soon after anthesis (Figure 1) (Bleecker and Patterson, 1997). At positions 2, 4, and 6 (counted from the first flower with visible white petals at the top of the inflorescence), the floral organs of wild-type as well as *etr1-1* and *ida* plants were turgid and attached to the developing silique (Figure 1B). At position 10, the perianth and stamens had abscised from the wild-type flower. The *etr1-1* mutant abscised its flowers first at position 16 (Figure 1B). By contrast, the mutant *ida* retained its floral parts indeterminately (past position 30; Figures 1A and 1C). After the shedding of mature seeds, the now completely dry, colorless, and transparent senesced floral parts of the mutant *ida* remained attached (Figure 1C).

Scanning electron microscopy was used to compare the morphology of wild-type petal AZ with that of *ida* and to discern possible changes in the petal AZ of *ida* (Figures 2A to 2J) after either forcible removal or natural abscission of the petals. At position 4, broken cells were revealed at the fracture plane of the petal AZ in the wild type and the *ida* mutant (Figures 2A and 2F). This was followed by the exposure of a flattened fracture plane at position 8 (Figures 2B and 2G), indicating the partial dissolution of the middle lamella in the petal AZ cells. At position 10, wild-type AZ cells started to show an initial rounded appearance (Figure 2C), whereas the fracture plane of *ida* still revealed only the flattened cavity (Figure 2H). The rounding and elongation of cells proceeded in the wild type, and cells were fully rounded by position 12 (Figure 2D). Although the cells of the fracture plane of *ida* seemed to follow a similar progression, these cells appeared to be more obscured by middle lamellar material and less rounded (Figure 2I) than wild-type cells at positions 10 and 12 (Figures 2C and 2D). At later stages, an increase in the number of broken cells was observed in *ida* (Figure 2J). These broken cells were highly similar to those seen in early positions and correlated with high breakstrength (Figures 2J and 2K; see below), indicating an incomplete dissolution of the middle lamella in AZ cells in *ida*.

To obtain a quantitative measure of the difference between the wild type and *ida*, the force needed to remove petals from

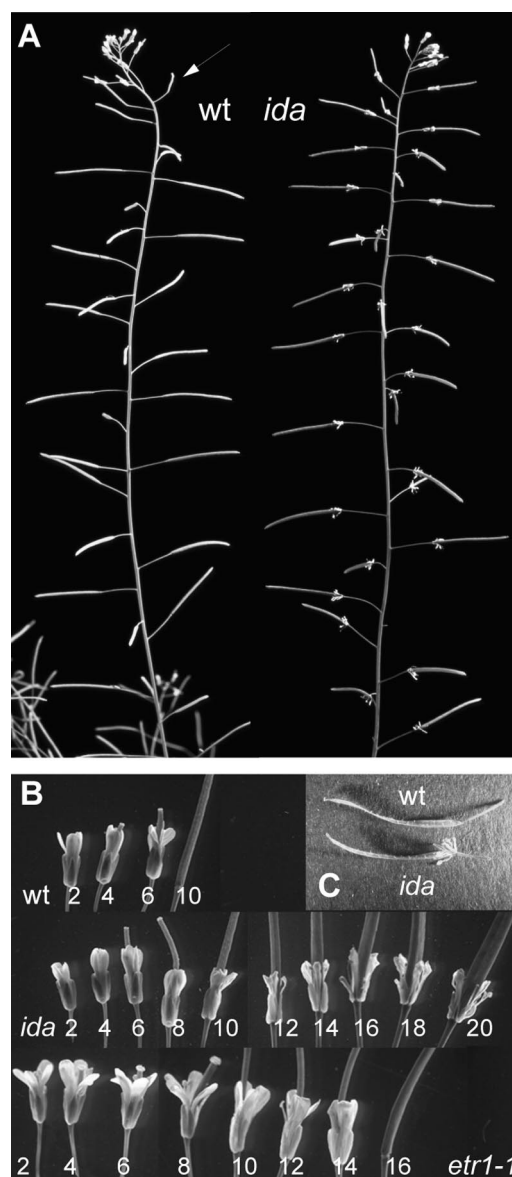


Figure 1. Phenotype of the *ida* Mutant Compared with the Wild Type and *etr1-1*.

(A) Inflorescences of wild-type (wt) *Arabidopsis* and the *ida* mutant. The arrowhead indicates the first wild-type flower position where the floral organs have abscised. Note *ida* flowers attached along the entire inflorescence.

(B) Flowers along the inflorescence. Note the indications of senescence in *ida* flowers from position 16, showing that the mutant is sensitive to ethylene. Note also fresh, turgid, and vivid floral organs at all positions before abscission in the ethylene-insensitive *etr1-1* mutant.

(C) Septum from a dry plant after dehiscence of seeds with dry floral organs still attached in the *ida* mutant, in contrast to the wild type.

the plant was measured using a stress transducer (Fernandez et al., 2000). As shown in Figure 2K, the breakstrength of wild-type petals decreased rapidly from position 2, in agreement with the scanning electron micrographs at the different positions. At position 8, the breakstrength was not measurable, and

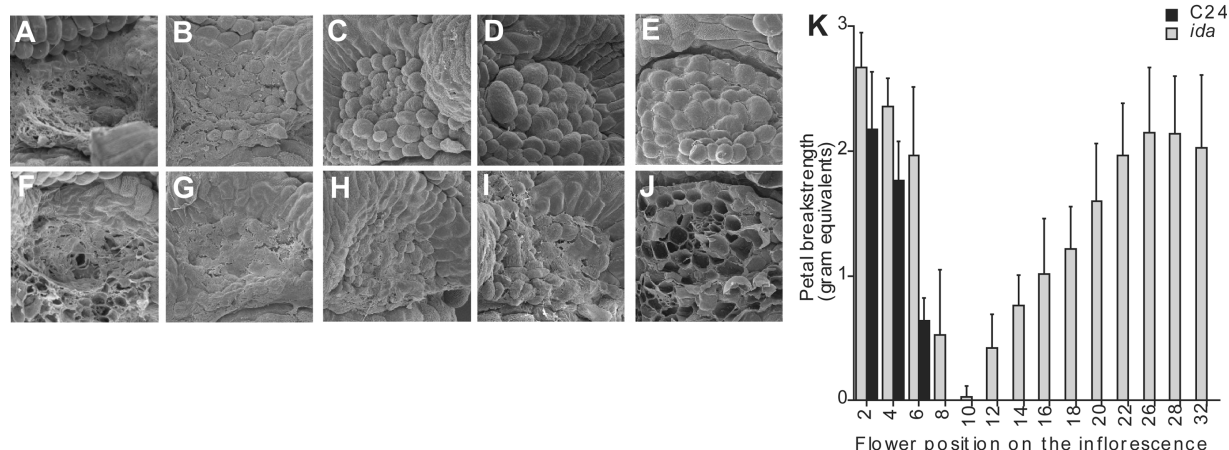


Figure 2. Morphology of AZs and Petal Breakstrength.

Scanning electron microscopy of the fracture plane AZ cells of petals in wild-type ([A] to [E]) and *ida* ([F] to [J]) flowers at positions 4 ([A] and [F]), 8 ([B] and [G]), 10 ([C] and [H]), 12 ([D] and [I]), and 22 ([E] and [J]) after forcible removal or natural abscission. Wild-type petals abscise naturally at position 8. ([K]) shows petal breakstrength (i.e., the force required to remove the petals from the flowers) measured from positions 2 to 32 along the inflorescence. Breakstrength was measured for 15 wild-type and *ida* plants, with a minimum of 20 measurements at each position. Standard deviations are shown as thin lines at the top of the columns.

the petals fell off at the slightest touch. The *ida* mutant initially showed a similar, but slightly delayed, breakstrength profile compared with the wild type. It is significant that at position 10 of the mutant, force still was needed for detachment, although the breakstrength approached zero. After position 12, the breakstrength increased again, in agreement with the increase in the number of broken cells observed. The oldest *ida* flowers on an inflorescence (position 32) had a breakstrength similar to that of the youngest flowers.

The *ida* Mutant Is Sensitive to Ethylene

In the *ida* mutant, no developmental processes other than floral abscission were affected. This is in contrast to the ethylene insensitive mutants *etr1* and *ein1*, which in addition to a delay in floral abscission showed delayed leaf senescence, larger rosettes, a delay in bolting and flowering, and very low seed germination rates under a variety of environmental conditions compared with wild-type plants (Bleecker et al., 1988; Guzman and Ecker, 1990; Grbic and Bleecker, 1995; Roman et al., 1995).

To investigate whether there were additional differences between *ida* and the ethylene-insensitive mutants, we tested the ethylene sensitivity of *ida*. In contrast to *etr1-1*, the *ida* mutant was sensitive to ethylene (Figure 3). The "triple-response" assay has been used to identify mutants altered in ethylene synthesis, perception, and responses (Kieber et al., 1993). Seedlings of the *ida* mutant germinated on the natural precursor of ethylene, 1-aminocyclopropane-1-carboxylic acid (data not shown), or exposed to ethylene at 10 ppm (Figure 3A) displayed the same drastic morphological changes characteristic of wild-type seedlings (i.e., inhibition of root and hypocotyl elongation, radial swelling of the hypocotyl and root, and exaggeration in the curvature of the apical hook). Thus, in contrast to *etr1-1* seedlings, *ida* seedlings seemed perfectly capable of perceiving and re-

sponding to ethylene. Similarly, incubation of mature plants in chambers with ethylene at 10 ppm resulted in wilting of rosettes and cauline leaves in wild-type and *ida* plants, whereas *etr1-1* plants were unaffected by the treatment (Figure 3B). In wild-type plants, this level of ethylene also resulted in senescence and abscission of floral organs soon after the opening of the flower. In the *ida* plants, floral organs senesced but did not abscise (Figure 3C). Thus, except with regard to floral abscission, *ida* reacted as a wild-type plant to ethylene exposure.

The *ida* Mutant Phenotype Is Caused by a Single Recessive Mutation

To identify the genetic basis for the *ida* phenotype, the mutant was crossed to wild-type *Arabidopsis*. F1 plants from the cross did not show the phenotype, indicating that *ida* is controlled by a recessive gene. In the F2 generation, the number of wild-type and *ida* plants was consistent with the 3:1 ratio (37 wild-type:11 *ida*; $\chi^2 = 0.13$, $P > 0.7$) that would be expected if the *ida* phenotype is the result of a homozygous recessive, monogenic mutation. The T-DNA of pMHA2 carries a marker gene (*npthII*) conferring kanamycin resistance (Mandal et al., 1995). All progeny plants displaying the *ida* phenotype were homozygous for the single T-DNA present in the *ida* mutant line (i.e., the progeny of *ida* plants were always 100% kanamycin resistant). The cosegregation of homozygosity of the T-DNA and the *ida* phenotype indicated that the T-DNA insertion caused the mutant phenotype.

The *ida* Mutant Is Rescued by a 2019-bp Genomic Fragment

The plant DNA flanking the right border of the T-DNA insertion was cloned using inverse PCR (Meza et al., 2002), whereas the other side was cloned by standard PCR with a T-DNA-specific

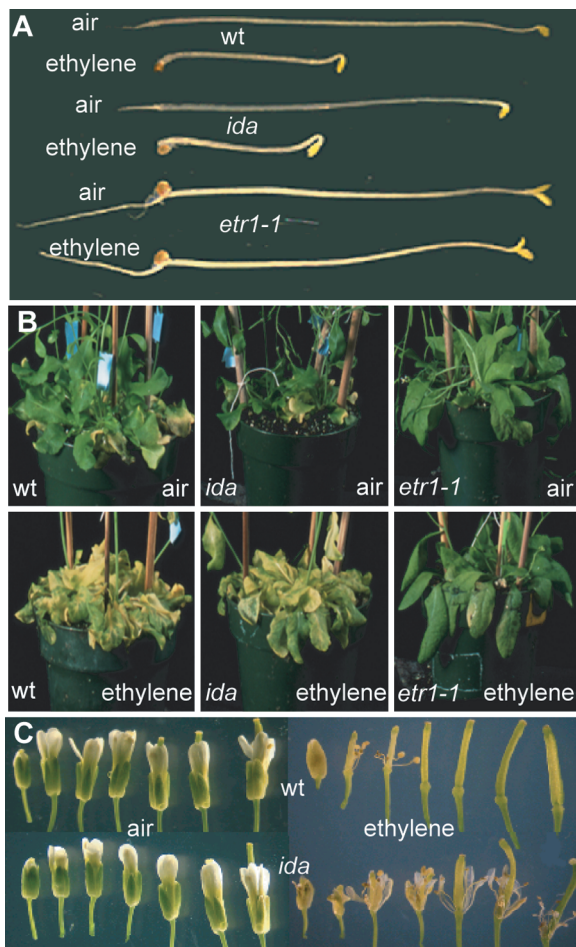


Figure 3. Ethylene Response of the *ida* Mutant.

(A) The triple-response assay was conducted by exposing seedlings growing on vertical half-strength Murashige and Skoog (1962) agar plates to 10 ppm ethylene for 3 days in the dark. Note that *ida* reacts as a wild-type (wt) seedling, whereas *etr1-1* is insensitive to ethylene and behaves like a control seedling subjected to air.

(B) Mature wild-type, *ida*, and *etr1-1* adult plants were exposed to 10 ppm ethylene for 48 h in flow-through chambers. Note the yellow, wilting rosette leaves of the wild type and *ida* but not of *etr1-1*.

(C) Comparison of flowers at positions 0 to 6 exposed to air or to 10 ppm ethylene. In wild-type flowers, exposure to ethylene causes senescence and floral organ abscission already in flowers at position 1. By contrast, *ida* flowers senesce but do not abscise.

primer and a genomic primer (see Methods). Sequencing of the cloned junctions revealed that the T-DNA was inserted on chromosome 1 between an annotated gene that encodes a putative protein with 10 LRRs (At1g68780) and a small, intronless gene (At1g68765) (Figure 4A).

To determine whether either of these genes was affected by the T-DNA insertion, we transformed *ida* mutant plants with two independent genomic fragments: one (2633 bp) covered the LRR gene, including 959 bp of upstream and 154 bp of downstream sequence; the other (2019 bp) started 8 bp downstream of the stop codon of the At1g68780 gene and ended 303 bp down-

stream of the At1g68765 open reading frame (Figure 4A). Fifty-nine and 58 independent transformants were generated for each construct, respectively. All of the transformants harboring the LRR gene displayed the mutant *ida* phenotype (Figure 4B), whereas 54 plants transformed with At1g68765 all showed a

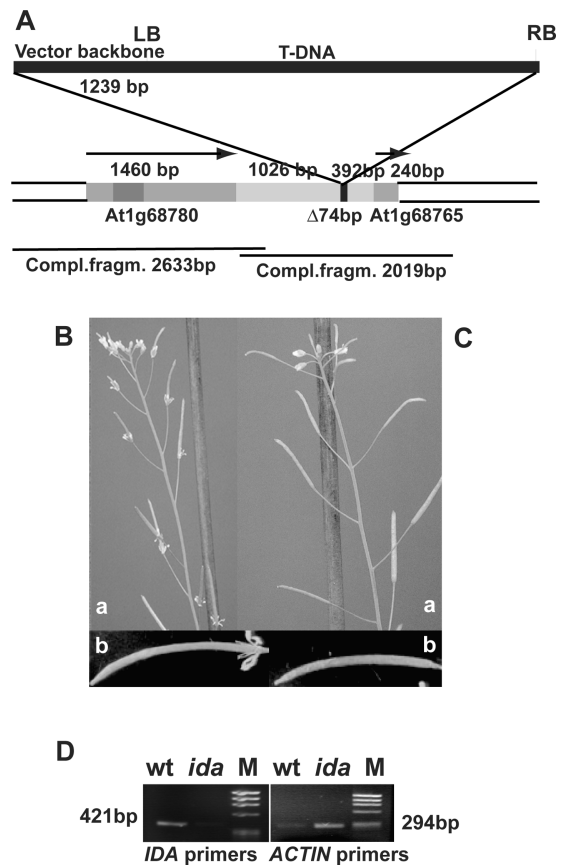


Figure 4. Identification of the *IDA* Gene.

(A) The single T-DNA with 1239 bp of vector backbone was inserted in chromosome 1 between genes At1g68780 and At1g68765 in the *ida* line. The T-DNA insertion had resulted in a 74-bp target-site deletion (Δ). The distances from the stop codon and the start codon of these two genes, respectively, to the T-DNA insertion point are shown (bp), as are the numbers of base pairs from the start to the stop codons in the two genes. The single intron in At1g68780 is indicated in black. The direction of transcription is indicated by arrows. The extents of the two genomic fragments used in a complementation experiment are shown below the genomic region. All elements in the drawing are not to scale.

(B) The phenotype of *ida* plants transformed with the fragment encompassing the At1g68780 gene was identical to the *ida* mutant phenotype (a). Note flowers attached to full-grown siliques (b).

(C) The phenotype of *ida* plants transformed with the fragment covering the At1g68780 gene was identical to the wild-type phenotype (a). Note that floral organs are absent from siliques in the lower positions of the inflorescence (b).

(D) RT-PCR on mRNA from flowers at positions 1 to 8 amplified the expected 421-bp fragment with *IDA* primers from wild-type (wt) but not from *ida* plants, whereas a 294-bp *ACTIN2-7* fragment was amplified from both wild-type and *ida* plants. M, φX174 digested with HaeIII.

wild-type abscission pattern (Figure 4C). Because the small open reading frame with its upstream and downstream sequences can complement the mutant phenotype, we concluded that we had identified the *IDA* gene.

A cDNA corresponding to the *IDA* gene, with a 98-bp 5' untranslated region and a 205-bp 3' untranslated region, was cloned recently. Therefore, the T-DNA in the *ida* mutant seems to be positioned in the promoter of the *IDA* gene (Figure 4A). Reverse transcriptase-mediated (RT) PCR on mRNA of flowers (positions 1 to 8) amplified the expected PCR fragment from wild-type but not from mutant tissue (Figure 4D), whereas *ACTIN2-7*, tested as a positive control, was amplified from both wild-type and *ida* first-strand cDNA templates (Figure 4D), and negative control experiments run without reverse transcriptase yielded no PCR products (data not shown). Thus, RT-PCR indicated that the T-DNA insertion had interfered with normal gene expression.

An *IDA*: β -Glucuronidase Reporter Is Expressed Specifically in Floral AZs

To investigate the expression pattern of the wild-type *IDA* gene, a promoter fragment of 1419 bp was cloned in a T-DNA vector in front of the β -glucuronidase (*GUS*; *uidA*) gene (see Methods).

Transformed *Arabidopsis* plants were investigated in a *GUS* assay for *IDA*:*GUS* reporter gene expression. Tissue from roots and all aerial parts of the plants was inspected, and expression was found to be confined exclusively to specific stages of flower development. An in-depth analysis was performed on selected T1 plants and their T2 siblings. These lines harbored multiple copies of the *IDA*:*GUS* construct, but no significant variation was found between the sublines. Developmental series of flowers were numbered corresponding to their positions on the inflorescence and stained for *GUS* activity (Figure 5A). Position 1 corresponded with anthesis, when carpels, anthers, and petals are of approximately similar lengths. *IDA*:*GUS* activity was absent in flowers from positions 1 to 4. At position 5, a strong *GUS* signal was detected in the floral organ AZ, concurrent with the decrease in petal breakstrength (Figure 5A). The specific AZ signal was maintained throughout the floral abscission process (Figure 5A).

GUS expression was restricted specifically to the AZ at the bases of all floral organs (filaments, petal, and sepals) at position 5. At mid-abscission stages (position 6), *IDA*:*GUS* expression was observed in the AZ of petals, sepals, and anther filaments on the plant body side (Figures 5A and 5D to 5F). In addition, both strong and weak expression were found in the

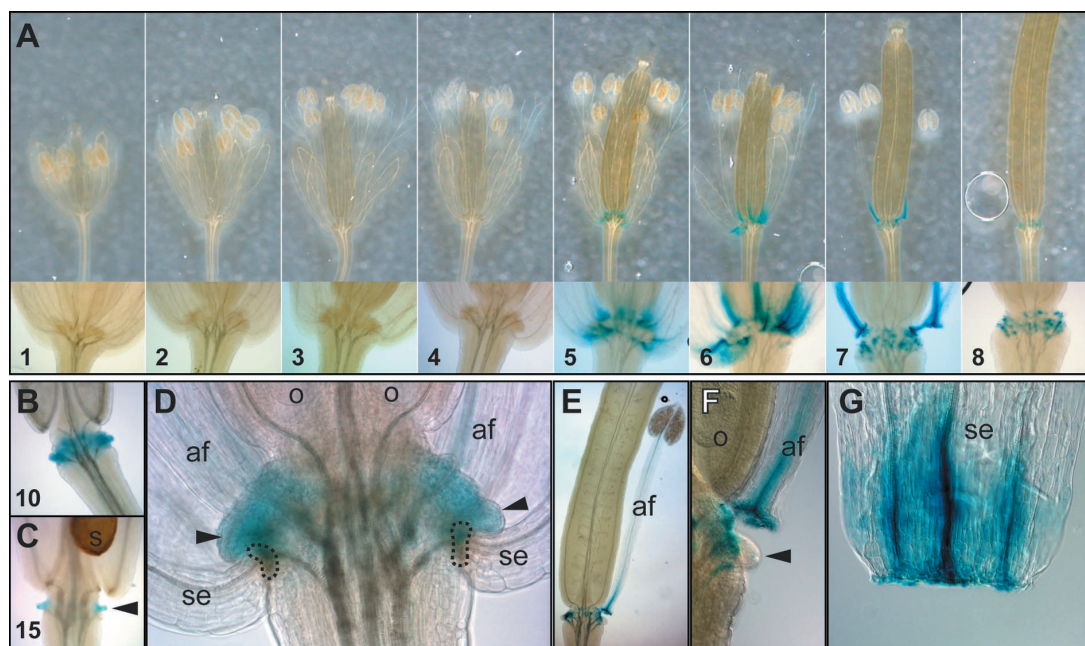


Figure 5. *IDA*:*GUS* Expression Assay.

Cleared whole-mount preparations of *GUS*-stained *IDA*:*GUS* flowers from different developmental stages.

(A) Developmental assay showing stage-specific AZ *GUS* expression in early *IDA*:*GUS* flower stages. Top row, whole-flower overview; bottom row, AZ detail. Arabic numerals indicate flower positions on the inflorescence.

(B) and (C) AZ *GUS* expression in flowers at positions 10 and 15. The arrowhead indicates nectary outgrowth. S, mature seed.

(D) *GUS* expression in the AZ (stippled lines) and in nectaries (arrowheads) between the sepal bases (se) and anther filament bases (af). O, ovule.

(E) *GUS* expression in the AZ and in the anther filament base.

(F) Detail of (E). Note the *GUS* expression in the anther filament AZs on both the plant body side and the anther filament side. The arrowhead marks nectary outgrowth with weak *GUS* expression.

(G) *IDA*:*GUS* expression in the sepal. The signal seems to diffuse from the base toward the sepal apex.

outgrowths of the nectary (Figures 5D and 5F, respectively). *IDA:GUS* expression also was observed through position 10, although all floral organs were abscised (Figure 5B). At later stages, at floral position 15, where the seeds are close to maturity, a prominent GUS signal still was found, although it was more or less restricted to the outgrowths of the medial portion of the nectary (Figure 5C). During the course of abscission, the GUS signal appeared to spread toward the petal, sepal, and filament apices, probably associated with the vascular tissue and most likely attributable to spreading of the product of the GUS reaction rather than to promoter activity (Figures 5A and 5E to 5G). Together, the observed *IDA:GUS* expression pattern and timing are congruent with the phenotypic changes seen in the *ida* mutant.

The *IDA* Gene Encodes a Protein with a Signal Peptide

The *IDA* gene encodes a small protein of 77 amino acids with an N-terminal hydrophobic region predicted by SignalP software to act as a signal peptide (Nielsen et al., 1997), whereas no trans-membrane region was detected. To investigate whether the *IDA* protein was secreted, we bombarded onion cells with constructs containing translational fusions between the *IDA* cDNA, or the putative signal peptide, and the green fluorescent protein (GFP) (see Methods). Both the *IDA:GFP* protein (Figure 6A) and the signal peptide:GFP fusion protein (Figure 6B) gave high GFP signals at the perimeter of a single cell; additionally, a slightly weaker GFP signal was found around neighboring cells. It appears that the fusion proteins spread out between the adjacent cells. By contrast, the signals from the GFP protein on its own and GFP fused to *Drosophila* Heterochromatin Protein1 (HP1), a positive control for subcellular targeting, never were seen in clusters of cells (Figures 6C and 6D), indicating that the signal always was restricted to the bombarded cell. GFP alone was present in the cytoplasm and diffused also into the nucleus as a result of its small size, as reported previously (von Arnim et al., 1998) (Figure 6C), whereas GFP:HP1 was found solely in the nucleus (Figure 6D). The subcellular localization assay suggests that the *IDA* and its signal peptide can export GFP through the secretory pathway of the bombarded cell to the extracellular (apoplastic) space, where it spreads to neighboring cells, and/or, assuming that several neighboring cells are transformed and express the fusion proteins, that *IDA* is localized to the plasma membrane.

IDA-LIKE Genes Are Present in Arabidopsis and Other Plant Species

The C-terminal 20 amino acids of the *IDA* protein was used in tBLASTn (Basic Local Alignment Search Tool) searches against plant EST collections, and *IDA-LIKE* (*IDL*) transcripts from eight different plant species, including one cDNA from Arabidopsis, were identified. These transcripts encode proteins that are similar to *IDA*—that is, they have predicted N-terminal signal sequences (using SignalP), similar pI values (ranging from 11.02 to 12.62; Table 1), and a conserved C-terminal signature (pv/iPpSa/gPSK/rk/rHN), which we have termed PIP (Figure 7A).

tBLASTn searches also were performed against the translated Arabidopsis genome. The hits found were inspected for

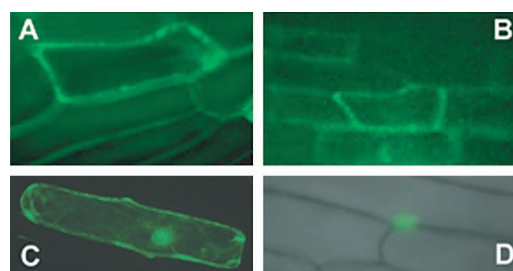


Figure 6. Subcellular Localization of Proteins in an Onion Epidermis Transient Expression Assay.

GFP fluorescence was revealed 2 h after bombardment using a Nikon Microphot microscope (Tokyo, Japan) equipped with epifluorescence and Nomarski optics.

(A) Fluorescence micrographs of the extracellular localization of the *IDA:GFP* fusion protein. Note the presence of GFP signal around several neighboring cells.

(B) Fluorescence micrographs of the extracellular localization of the *IDA* signal peptide:GFP fusion protein. Note the presence of GFP signal around several neighboring cells.

(C) Fluorescence micrographs of the cytoplasmic localization of GFP alone. The signal in the nucleus is the result of diffusion of the small GFP protein (~25 kD) (von Arnim et al., 1998). Note that the GFP signal is not seen in neighboring cells.

(D) Merged fluorescence and differential interference contrast micrographs of the nuclear localization of the GFP:HP1 fusion protein, a control for subcellular localization. Note that the GFP signal is not seen in neighboring cells.

short open reading frames encoding proteins with predicted signal peptides and similarity to *IDA* in the C-terminal end. This procedure led to the identification of four additional putative *IDL* genes encoding proteins of <100 amino acids that to date are unannotated (Figure 7A, Table 1). The putative encoded proteins also have high pI values (10.18 to 12.52; Table 1).

The *IDL* proteins can be divided into two subclasses: AtIDL2 to AtIDL5 and the IDL1s from poplar, wheat, and maize have a conserved Gly residue very close to the C-terminal end that is lacking from the other proteins (Figure 7A). The 30 to 40 amino acids just after the signal peptide are less well conserved than the PIP motif. However, similarities are found in this region across species (e.g., AtIDL2 and AtIDL3 and the PtIDL1 of poplar; ZmIDL1 and TaIDL1 of maize and wheat; and the IDL1 proteins of lotus, soybean, and black locust). The expression pattern of the *IDL* mRNAs identified in the databases have not been investigated. However, the cDNA libraries they come from (e.g., pathogen-infected plants, petioles, and sapwood-heartwood transition zones; Table 1) indicate that *IDL* proteins may function in diverse environmental and developmental processes.

To investigate whether the four unannotated putative Arabidopsis *IDL* genes were expressed, RT-PCR was performed on first-strand cDNA generated from mRNA of different tissues (Figure 7B). *AtIDL1* also was included in our study. mRNA was isolated using magnetic oligo(dT) beads (see Methods), and the *ACTIN* primers used to control the quality and amount of first-strand cDNA amplified the expected fragment at similar levels from the six tissues tested (Figure 7B). Negative control experi-

Table 1. Features of *IDL* Genes and cDNAs and Their Encoded Proteins

Protein Name	Protein Identifier/ cDNA Accession Number	Gene/BAC Clone	BAC Clone Position	Chr ^a	pI ^b	Tissue Source of cDNAs/ Expression Pattern
IDA	AAM65435.1	At1g68765		I	11.87	See Figure 5
AtIDL1	AAM63318.1	At3g25655		III	12.24	Top-most inflorescence tissues and roots; see also Figure 7B
AtIDL2		MUB3	69965 to 70249	V	12.52	See Figure 7B
AtIDL3		F17114	1503 to 1207	V	10.61	See Figure 7B
AtIDL4		MVE11	24901 to 25179	III	11.92	See Figure 7B
AtIDL5		F22K20	33903 to 33595	I	10.18	See Figure 7B
GmIDL1	BQ630646				11.74	Roots
LeIDL1	AI779570				11.02	<i>Pseudomonas</i> -susceptible tomato
LjIDL1	AW719486				11.13	Nodules
PtIDL1	BU889756				12.53	Petioles
RpIDL1	BI642538				11.42	Sapwood/heartwood transition zone
TaIDL1	BM135459				11.37	<i>Fusarium graminearum</i> -infected spikes
ZmIDL1	BI430572				12.62	Juvenile vegetative shoots

^a Arabidopsis chromosome.

^b pI values of proteins without putative N-terminal signal peptides, as calculated by Isoelectric⁺ from the Genetics Computer Group.

ments performed for all primer pairs without reverse transcriptase yielded no PCR products (results shown for *ACTIN*; Figure 7B).

The *AtIDL1* cDNA clone was isolated from an inflorescence and root library; accordingly, the transcript was amplified from roots. *AtIDL2* was expressed mainly in the aerial parts of the plant (i.e., rosette leaves, buds, flowers, and seedlings), but weak PCR fragments also were detectable in roots and mature seeds. *AtIDL3* was expressed only in flowers and seedlings. *AtIDL4* and *AtIDL5* have a similar stretch of amino acids between the signal peptide and the PIP motif (Figure 7A), and these genes showed similar expression profiles (i.e., they were both expressed in buds, flowers, and seedlings), but *AtIDL4* also was expressed in roots. At best, the RT-PCR method is semiquantitative, but given the even amplification of the *ACTIN2-7* transcript in all tissues, our experiment suggests that the five *AtIDL* genes have expression patterns distinct from that of *IDA*, which is detected only in AZ (Figure 5). Thus, the encoded proteins are suggested to be involved in other developmental processes than is *IDA*.

DISCUSSION

The *ida* Mutant Is Unique in That Floral Organs Are Completely Deficient in Abscission

A variety of mutants, including the recently identified *delayed abscission* mutants in *Arabidopsis* (*dab1* to *dab5*), show a visible delay in floral abscission compared with wild-type flowers (Lanahan et al., 1994; Bleecker and Patterson, 1997; Wilkinson et al., 1997; Patterson, 2001). The mutant *ida* is different from any other abscission mutant described previously in that its floral parts still remain attached to the plant when it undergoes the normal monocarpic senescence process (Figure 1C). Therefore, we describe *ida* as a mutant deficient, rather than delayed, in floral abscission. The normal opening and dehiscence of the valves and the shedding of seeds from the false septum of *ida* strongly indicate that the mutation disrupts a pathway specific to the control of floral abscission rather than a more generalized regulation of cell separation.

The *IDA* Gene Is Suggested to Be Involved in an Ethylene-Independent Developmental Pathway That Controls Floral Abscission

The involvement of ethylene in abscission has been widely documented (Sexton et al., 1985), and until recently (cf. the *dab* mutants [Patterson, 2001]), all mutants delayed in floral abscission were deficient in ethylene perception (Bleecker et al., 1988; Lanahan et al., 1994; Payton et al., 1996; Bleecker and Patterson, 1997; Wilkinson et al., 1997). *ida*, however, is not ethylene insensitive: seedlings of the *ida* mutant showed the same triple response as wild-type seedlings (Figure 3A). In addition, adult *ida* plants responded with senescence of leaves and flowers when exposed to ethylene (Figures 3B and 3C). However, the presence of ethylene does not induce any floral abscission process in the *ida* mutant, in clear contrast to the acceleration of the abscission process in wild-type plants exposed to ethylene (Figure 3C).

Because *ida* has an ethylene-independent block in floral abscission but is otherwise sensitive to ethylene, we suggest that *IDA* is involved in an ethylene-independent developmental pathway that controls this process. This pathway also may involve HAESA and AGL15, which influence abscission but not ethylene sensitivity (Fernandez et al., 2000; Jinn et al., 2000). If *IDA* is regulated solely by ethylene, one would expect the *etr1* mutant to be completely deficient in abscission, but this is not the case. However, because the timing of abscission clearly can be modified by ethylene, we cannot eliminate the possibility that ethylene is involved indirectly in inducing the *IDA* function. Therefore, it will be of interest to cross *IDA:GUS* plants to *etr1* mutants. It is reasonable to suggest that *IDA* and *ETR1* may act in parallel pathways to control the expression of genes that contribute to abscission.

The *ida* Mutation Disrupts the Separation Step of Floral Abscission

The breakstrength data, as well as the petal AZ fracture planes seen in the scanning electron micrographs (Figure 2), suggest that the initial steps in the abscission process are only delayed

in the *ida* mutant, whereas the major effect of the mutation is seen at the stage at which separation of the floral organs from the main body of the plant normally would have occurred.

The presence of a flattened fracture plane rather than broken cells indicates a partial dissolution of the middle lamella. When petals are removed forcibly, broken cells often result, as is seen for wild-type and *ida* plants at position 4 (Figures 2A and 2F). This results from the greater cell adhesion strength between the AZ

cells than in the tissues of the developing petal. It is evident that in *ida*, early changes in the middle lamella that result in loosening of the cell-to-cell adhesion must occur, and this is substantiated by observing the flattened fracture plane at positions 8 and 10 (Figures 2G and 2H) and changes in breakstrength (Figure 2K). The initial dissolution of the middle lamella is followed by loosening of the cell wall, and these changes coincide with an elongation and rounding of the AZ cells at the fracture plane, as seen for wild-type

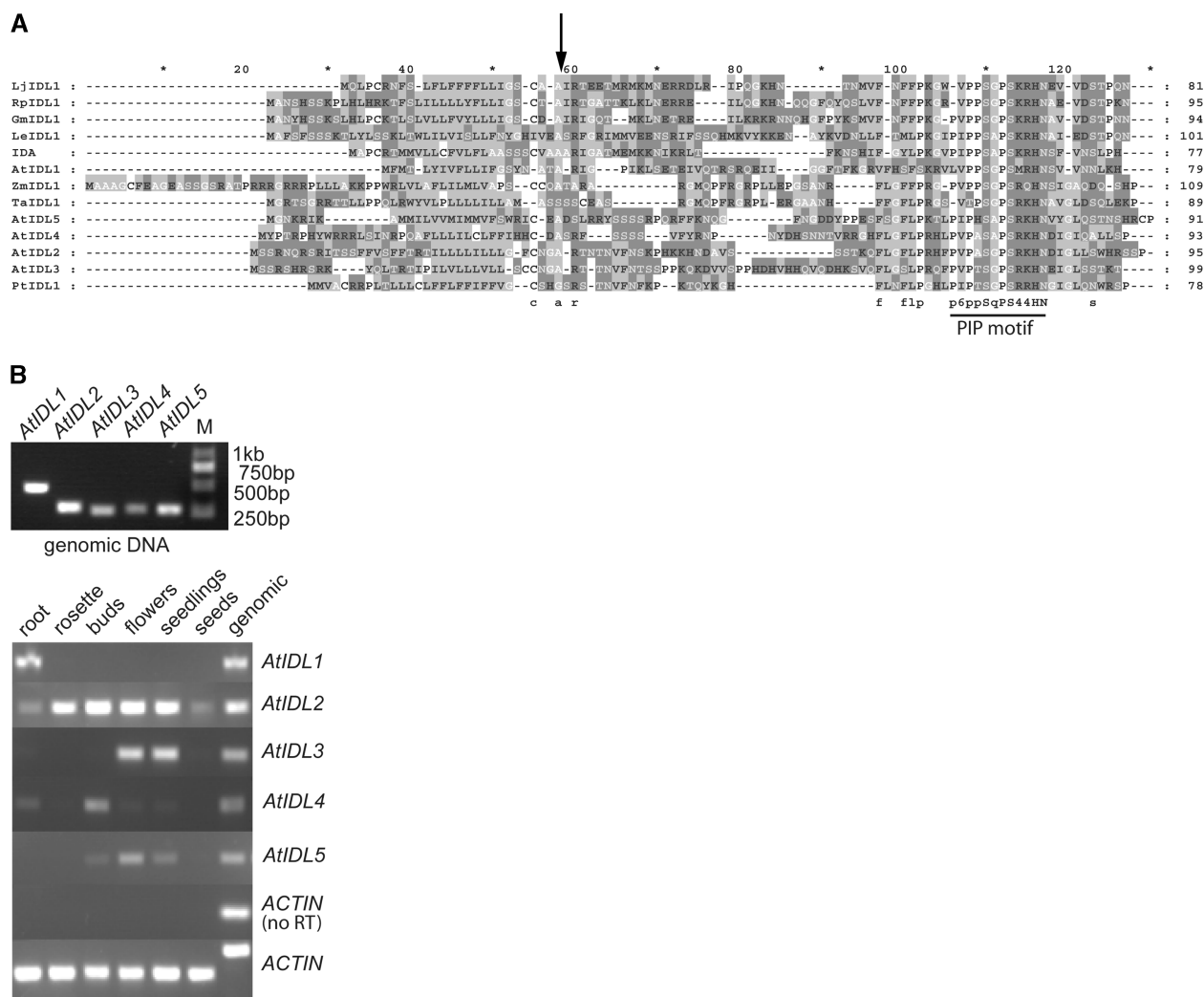


Figure 7. Proteins Encoded by *IDL* Genes and Expression Patterns in Arabidopsis.

(A) Alignment of IDA and IDL proteins encoded by cDNAs from Arabidopsis (AtIDL1), tomato (LeIDL1), lotus (LjIDL1), soybean (GmIDL1), black locust (RpIDL1), maize (ZmIDL1), poplar (PtIDL1), wheat (TaIDL1), and four putative IDL genes of Arabidopsis (see Table 1). Note the hydrophobic predicted signal peptides and the arrow indicating the positions of cleavage sites predicted by SignalP. Amino acids are shaded according to properties: light gray with dark letters, hydrophobic residues; dark gray with dark letters, basic residues; light gray with white letters, small residues; dark gray with white letters, polar nonaliphatic residues. The best conserved residues are shown below the alignment: uppercase letters, amino acids identical in all proteins; lowercase letters, amino acids identical in at least eight proteins; 6, hydrophobic residue (Val or Ile); 4, positive residue (Lys or Arg). The conserved PIP motif is indicated.

(B) RT-PCR on mRNA from different tissues, as indicated (bottom gels), using primers amplifying fragments of 465 bp (AtIDL1), 280 bp (AtIDL2), 256 bp (AtIDL3), 261 bp (AtIDL4), and 259 bp (AtIDL5). At top, genomic DNA was used as a template, and the marker line (M) is shown. Note that the positive control for *ACTIN*2-7, giving a fragment of 255 bp with primers spanning intron 2, was amplified at comparable levels from all tissues. Note also that the negative control PCR gel—*ACTIN* (no RT)—shows no products except for the *ACTIN*2-7 genomic control of 340 bp.

plants at positions 10 and 12 (Figures 2C and 2D). *ida*, on the other hand, shows only an initial rounding of the AZ cells (Figure 2I), indicating the commencement of dissolution of the middle lamella between adjacent AZ cells. Because fully rounded cells are not observed in the *ida* mutant and breakstrength measurements never reach zero, we propose that *ida* is defective in cell wall dissociation between AZ cells and therefore never reaches the point of floral organ detachment.

The *ida* mutant phenotype has enabled us to refine our working model for the abscission process (Patterson, 2001). First, the AZ is formed at the base of the organ to be shed. Obviously, mutants deficient in the formation of an AZ, like the *jointless* mutant in tomato, cannot go through abscission (Mao et al., 2000). However, the *ida* mutant demonstrates that the development of an AZ is not sufficient for abscission to take place.

In the second stage of abscission, the AZ is presumed to acquire the competence to respond to abscission signals. In responsive AZs, ethylene can speed up the activation of the abscission process, as seen for wild-type flowers (Figure 3C). However, the ethylene-sensitive *ida* mutant shows that ethylene itself is not sufficient for abscission to occur.

The abscission process involves a maturation stage with changes in cell extensibility and elongation, followed by the actual dissolution of the middle lamellae between the cells on the main body of the plant and the organ to be shed. The initial decrease in petal breakstrength and the tendencies of rounding of cells in the AZ (position 12) of the *ida* mutant (Figures 2I and 2K) indicate that these aspects of AZ maturation are not sufficient for abscission to occur. Thus, the final separation step, cell wall dissociation, represents a distinct stage in the abscission process. According to our data, the *ida* mutant is deficient at this stage: without a functional *IDA* gene, this final stage of the abscission process will not take place.

Based on the features of the encoded protein (Figures 6 and 7A) and the restricted expression of *IDA* solely in the floral AZs, we suggest that *IDA* is involved in an abscission-specific signaling pathway that leads to, or enables, cell separation. Indeed, the Arabidopsis plasma membrane-associated LRR-RLK HAESA has been shown to be involved in the control of floral organ abscission (Jinn et al., 2000), and it would be interesting to investigate whether *IDA* could function as a ligand for HAESA.

IDA could act either in a positive signaling pathway, inducing genes involved in the final separation step, or alternatively in a negative signaling pathway, inhibiting a repair process potentially induced in the AZ by the initial dissolution of the middle lamella. One can imagine that weakening of connections between cells normally would induce repair processes. For abscission to occur, such repair must be prevented. *IDA* might function in blocking repair, whereas in the *ida* mutant, the loosening of the middle lamella could trigger the repair process, explaining the increase in breakstrength from position 12 (Figure 2C).

The Spatial and Temporal Activities of the *IDA* Promoter Are Consistent with an Involvement of the Cloned *IDA* Gene in Floral Abscission

The single T-DNA of the *ida* line was shown to reside between two putative genes, but only the fragment containing the At1g68765

gene, and not the fragment covering the LRR gene, could complement the mutation (Figure 4). Therefore, At1g68765 was identified as the *IDA* gene. Four of 58 plants shown by PCR to contain the At1g68765 fragment still showed the *ida* phenotype. It is well known that the level of transgene expression is influenced by position effects and copy number. Thus, we assume that the expression level from the *IDA* gene in these four plants was not sufficient to achieve complementation.

Consistent with the involvement of *IDA* in floral abscission, RT-PCR showed that *IDA* expression was detected in wild-type but not in mutant flowers (Figure 4D). The *IDA::GUS* pattern (Figure 5) also is consistent with a role of the *IDA* gene in abscission. *IDA::GUS* expression was initiated specifically at developmental flower stages corresponding to floral position 5. This is concurrent with the initiation of floral abscission and suggests that *IDA* is upregulated from not present or nondetectable transcription levels at this stage. *IDA::GUS* expression is maintained at high levels throughout the abscission process and also is found in both plants and AZs of organs to be shed, supporting the hypothesis that *IDA* functions as an abscission-specific signal. The absence of *IDA::GUS* expression during the dehiscence of seeds as well as the normal shedding of seeds in the *ida* mutant also support this notion. The observed maintained *IDA::GUS* staining pattern in the floral AZs and in the outgrowths of the medial and lateral regions of the nectary (Figure 5) suggest that *IDA* also serves as a signal for postabscission processes. The nectary is known to aid in the secretion of a protective layer covering abscised cells after shedding of the floral organs (Bowman, 1994), and *IDA* in combination with other factors might function as a trigger in this process.

The *IDA::GUS* reporter construct may be valuable in future studies of abscission and AZ development. The *IDA* promoter has now been shown to be AZ specific. Previously, the promoters of a basic chitinase gene and a β -1,3-glucanase from bean coupled to the GUS reporter (*CHIT::GUS* and *GLUC::GUS*) were used as marker genes for abscission in Arabidopsis (Chen and Bleecker, 1995; Bleecker and Patterson, 1997; Patterson, 2001). In wild-type plants, *IDA::GUS* and *CHIT::GUS* seem to have temporally overlapping expression patterns (positions 5 to 8). It remains to be determined whether these promoters are expressed differentially in abscission mutants.

IDA and *IDL* Proteins Are Suggested to Represent a Novel Family of Ligands in Plants

Investigation of subcellular localization using the onion epidermis assay substantiated the notion that the N-terminal hydrophobic part of the small *IDA* protein is a signal peptide (Figure 6), as predicted by SignalP software. The signal peptide, small size, and high pI (11.87) are features similar to those of the ligand CLAVATA3 (CLV3), which is required to hinder the overproduction of flowers and floral organs in conjunction with the receptors CLV1 and CLV2 (Rojo et al., 2002). A large family of *CLV3-LIKE* (*CLE*) genes was identified recently by iterative BLAST searches in the Arabidopsis genome (Cock and McCormick, 2001). CLV3 and the *CLE* proteins have a common C-terminal motif. *CLE::GFP* fusions in the onion epidermis assay have been reported to spread to the perimeter of cells

adjacent to a bombarded cell (Sharma et al., 2003), and our results for GFP coupled to the whole IDA protein or its predicted signal peptide can be interpreted similarly (Figures 6A and 6B). No other hydrophobic regions apart from the predicted signal peptide are found in IDA, indicating that it is a soluble protein. Because no retention or sorting signal apparently is present in the IDA protein and the IDA protein seems to be localized to the extracellular space, we predict that IDA is exported through the secretory pathway by the default pathway for soluble proteins. However, our onion localization experiment cannot exclude the possibility that IDA is localized in the plasma membrane.

Proteins similar to the ligand of the *Brassica* S-locus receptor kinase, the S locus Cys-rich protein (SCR), are thought to represent a second class of plant ligands (Vanoothuyse et al., 2001). Both the CLE and the SCR-Like (SCRL) proteins are believed to interact with RLKs. The C terminus of the IDA protein is distinct from the CLE motif and the Cys-rich pattern of SCRLs; therefore, IDA is not a member of these two classes of putative ligands.

We have identified cDNAs that encode proteins with features similar to those of IDA in eight different plant species (Figure 7A). In addition, we have shown by RT-PCR that the putative *AtIDL* genes 2 to 5 are active genes expressed in diverse tissues (Figure 7B). Compared with the amplification of the *ACTIN2-7* transcript, these four genes, as well as *AtIDL1*, can be said to be expressed differentially. The *AtIDL1* transcript was amplified only in root tissue and may have a specific role in root development. *AtIDL2* was present in all tissues examined, but it seems to be expressed at a relatively higher level in the aerial parts of the plant. *AtIDL4* and *AtIDL5* seem to be expressed at relatively higher levels in buds and flowers, respectively, and may have specific functions in floral development. The differential expression pattern suggests that the members of this new family of genes may be important in diverse developmental processes in the plant.

The expression patterns of the *CLE* genes have been investigated using the same RT-PCR approach (Sharma et al., 2003). Approximately one-third of these genes are expressed ubiquitously, whereas the others have a more restricted expression pattern (e.g., *CLE2*, which is similar to *AtIDL4* in that it is expressed in roots, seedlings, and reproductive shoot apices/buds). By contrast, both *IDA* and *CLV3* have very constrained expression patterns, *IDA* in the AZ (Figure 5) and *CLV3* in the apical meristem (Fletcher et al., 1999).

Only a few ligand receptor pairs have been identified to date in *Arabidopsis*: ligands are known for BRI1 that are involved in hormone sensing (Li and Chory, 1997), for FLS2 that mediate the defense response (Gomez-Gomez and Boller, 2000), and for CLV1 (Rojo et al., 2002). However, in the *Arabidopsis* genome, there are >400 RLKs with a wide array of extracellular ligand binding regions (Shiu and Bleecker, 2001), signifying the presence of various and numerous ligands. To date, the CLE and SCRL classes of putative plant ligands have been characterized. The C-terminal amino acid sequence of IDA is distinct from both of these classes and similar to that of the group of IDL proteins putatively encoded by at least five genes in *Arabidopsis* and cDNAs of a diverse group of other plant species. Thus, we suggest that IDA and IDL proteins represent a third

class of partners of plant receptors. To understand the abscission process and other processes in which signaling networks are involved, it will be important to substantiate this hypothesis (e.g., by identifying the putative receptors of IDA and IDL proteins).

METHODS

Ethylene Responses

Wild-type (C24) and mutant *Arabidopsis thaliana* plants were analyzed for ethylene responsiveness by treating germinated seedlings with 10 ppm ethylene for 3 days in the dark (Chen and Bleecker, 1995) and gas-sing mature plants with 10 ppm ethylene for 48 h in a 16-h-day/8-h-night cycle.

Scanning Electron Microscopy

Individual flowers were fixed in 4% glutaraldehyde (w/v) in 0.5 M potassium phosphate buffer, pH 7.5, rinsed four times in buffer, and then dehydrated in a graded ethanol series. Samples were critical point dried in liquid CO₂ and mounted on steel plates covered with double-stick tape and sputter-coated with gold palladium. Samples were viewed at 10K accelerating voltage on a Hitachi S-570 scanning electron microscope (Tokyo, Japan).

Cloning of Plant DNA Flanking the T-DNA Insertion of the *ida* Line

The right border junction was cloned using inverse PCR (Meza et al., 2002) with *gus* 78 (5'-CACGGGTGTTGGGTTTCT-3') and *gus* 330 (5'-TGCGGTCACTCATTACGG-3') as a first primer set and *gus* 64L (5'-TTTCTACAGGACGGACCAT-3') and *gus* 342 (5'-TTACGGCAAAGTGTGGGTC-3') as a nested primer set. After sequencing of the amplified fragment, a genomic primer (*ida*49; 5'-GGTGTCTACTATGCGTGTG-3') and a left border-specific primer (5074+; 5'-ATTTGTCGTTTTATC-AAAATGTAC-3') were used in PCR to amplify the other junction.

Plant Material and Constructs for Complementation of the *ida* Mutation

Wild-type (C24) and transgenic *Arabidopsis* plants were cultivated in growth chambers at 22°C for 8 h of dark and 16 h of light (100 $\mu\text{E}\cdot\text{m}^{-2}\cdot\text{s}^{-1}$). Two fragments were used for a complementation test. A fragment encompassing the At1g68765 gene, amplified from genomic wild-type DNA using the primers 5'-GCTCTAGATGACCTATTTGAGAAAGACGAATG-3' and 5'-TCCCCCGGGTTCTGAATCAAAGGGTTTGTG-3', which have restriction endonuclease sites for XbaI and SmaI (in boldface), respectively, at the 5' ends, was inserted between the XbaI and SmaI sites of the Ti vector pGSC1704 (kindly provided by the Laboratory of Genetics, Flanders Interuniversity Institute for Biotechnology, Gent, Belgium), which has a hygromycin resistance gene within the T-DNA. A second fragment encompassing At1g68780 was amplified with primers with XbaI sites at the ends (5'-GCTCTAGATTTTGAAGAAAGGGACAGTTG-3' and 5'-GCTCTAGAGAACCGACCGTATCATACATTG-3') and cloned into the XbaI site of pGSC1704. *ida* mutant plants were transformed using the *Agrobacterium tumefaciens*-mediated floral dip method (Clough and Bent, 1998), and transformants were selected by germinating seeds on plates containing 10 $\mu\text{g}/\text{mL}$ hygromycin. PCR with construct-specific primers was used to confirm that resistant plants harbored the intended T-DNAs.

Reverse Transcriptase-Mediated Expression Analyses

mRNA was isolated from Arabidopsis tissues using magnetic oligo(dT) beads (GenoPrep mRNA beads; GenoVision, Qiagen, Valencia, CA) and treated with 1 unit of DNaseI (Invitrogen, Carlsbad, CA) per microgram of mRNA for 15 min at room temperature before first-strand cDNA synthesis with reverse transcriptase from *Avian myeloblastosis virus* (Promega) according to the manufacturer's suggestions. Negative controls were used in experiments in which the reverse transcriptase was omitted. The following gene-specific primers were used for PCR amplification from the cDNA: for *IDA*, 5'-GAAGAAAAAATTCGACTCCA-3' and 5'-TGGCCGTAATGACCTTAAAC-3'; for *ACTIN2-7*, 5'-GCTGGTTTTCGTGGT-GATGATG-3' and 5'-TAGAACTGGGTGCTCCTCAGGG-3' or 5'-CCGCAAGATCAAGACGAAGGATAGC-3' and 5'-CCCTGAGGAGCACCCAGTTCTACTC-3' spanning intron 2; for *AtIDL1*, 5'-AATAGCTAAATTAGTGTCTCCTCCTC-3' and 5'-AACGTTCCAACCGAGATATTAC-3'; for *AtIDL2*, 5'-CGTCTCGAAACCAAGATCAAG-3' and 5'-GGAGAAGATCGATGCCAAC-3'; for *AtIDL3*, 5'-TTTCGTGAAGGACCAGAAGTTG-3' and 5'-CTCGAAGCCACCGATCAAG-3'; for *AtIDL4*, 5'-CGTCCACATATTGGAGAAGAAG-3' and 5'-CAACAAGGCTTGAATACCAATG-3'; and for *AtIDL5*, 5'-TCATGGACATCTATGGAGTTAG-3' and 5'-GGTGTCTCATGGAGGATTGG-3'. For *IDA*, *ACTIN2-7*, *AtIDL1*, *AtIDL3*, and *AtIDL5*, PCR was run for 30 cycles; for *AtIDL2*, *AtIDL4*, and *ACTIN2-7* using the primers spanning intron 2, PCR was run for 35 cycles.

Generation of Transgenic *IDA:GUS* Plants

The *IDA:GUS* construct was made using Gateway cloning technology (Invitrogen). The pPZP211G vector is a pPZP Agrobacterium binary vector (Hajdukiewicz et al., 1994) with a spectinomycin bacterial selectable marker, *nptII*, as a plant selectable marker and a promoterless *GUS* gene with a *nos* terminator inserted between the *Sma*I and *Eco*RI sites of the polylinker. This vector was converted to a Gateway vector by inserting the C.1 Gateway cassette into the *Sma*I site in front of the *GUS* (*uidA*) gene using the Gateway vector conversion system (Invitrogen), thus generating the Gateway vector pPZP211G-GAWI. A 1419-bp *IDA* promoter fragment was amplified by PCR with the primers proA (5'-TTT-TCAATTTTGTATTGCAT-3') and proB (5'-ATTTGGTAGTCAATGTTTTT-TTC-3') with additional Gateway *att* sequences at the 5' ends introduced into the pDONR201 Gateway entry vector and thereafter recombined into the pPZP211G-GAWI vector, generating the construct pPZP *IDA:GUS*.

The construct was transferred to the *A. tumefaciens* strain C58C1 pGV2260 and used to transform Arabidopsis (ecotype C24) as described. Transformants were selected on Murashige and Skoog (1962) medium with 50 μ g/mL kanamycin. PCR with construct-specific primers was used to confirm that kanamycin-resistant plants were true transformants.

Histochemical GUS Assay

GUS staining, postfixation, and whole-mount clearing preparations of flowers and siliques from various positions along the inflorescence were performed as described (Grini et al., 2002) and inspected with a Zeiss Axioplan2 imaging microscope equipped with differential interference contrast optics and a cooled Axiocam camera imaging system (Jena, Germany).

Subcellular Localization Assay

For onion epidermis nuclear localization assays (Baumbusch et al., 2001), a cDNA-GFP fusion vector was made using Gateway cloning technology (Invitrogen). The pKEx-327 vector (Baumbusch et al., 2001) was converted to a Gateway vector (pKEGAW-smGFP) by inserting the C.1 Gateway cassette into a blunted *Sall* site using the Gateway vector

conversion system (Invitrogen). The coding region and the region encoding the amino acids encompassing the putative signal peptide, both with a 96-bp 5' untranslated region, were amplified with the primers *idaGFP*A (5'-TTATTCATTTCATTATAAGACCCTTC-3') plus *idaGFPD* (5'-ATG-AGGAAGAGAGTAAACAAAAGAG-3') and *idaGFP*A plus *idaGFPE* (5'-ACA-AGAACTACTCGCCGC-3'), respectively, with additional Gateway *att* sequences at the 5' end, and recombined into pKEGAW-smGFP so that the *IDA* coding region or signal peptide would be expressed as fusion proteins with the GFP at the C-terminal end. A GFP fusion construct with *Heterochromatin Protein 1* from *Drosophila melanogaster* in the pKEx-327 vector was used as a control for subcellular localization.

Bioinformatics Tools

Database searches were performed using BLASTP, tBLASTn, and PSI-BLAST (Basic Local Alignment Search Tool) (<http://www.ncbi.nlm.nih.gov/BLAST/>). The presence of an N-terminal signal peptide was investigated using SignalP (<http://www.cbs.dtu.dk/services/SignalP/>). Amino acid sequence alignments were created using CLUSTAL X 1.8 (<http://www-igbmc.u-strasbg.fr/BioInfo/ClustalX>) with default parameters and manual adjustments with GeneDoc 2.6.001 (<http://www.psc.edu/biomed/genedoc/>).

Upon request, materials integral to the findings presented in this publication will be made available in a timely manner to all investigators on similar terms for noncommercial research purposes. To obtain materials, please contact Reidunn B. Aalen, reidunn.aalen@bio.uio.no.

Accession Number

The accession number for the *IDA* cDNA is AY087883.

ACKNOWLEDGMENTS

We thank Fernando Rodriguez and Brad Binder for assistance with ethylene exposure of plants, Phil Oshel for assistance with scanning electron microscopy, Shinhan Shiu for constructive comments and suggestions to the article, Gunter Reuter for the pKEx-35S:*HP1:GFP* construct, Wuyi Wang for the pPZP211G vector, the Laboratory of Genetics of the Flanders Interuniversity Institute for Biotechnology for the pGSC1704 vector, Claudia Lipke for photography of plant samples, and Solveig Hauge Engebretsen, Roy Falleth, and Kirsten E. Rakkestad for technical assistance. This work was supported by Grant 129525/420 from the Research Council of Norway and U.S. Department of Agriculture Grant 00-35301-9085.

Received June 3, 2003; accepted July 18, 2003.

REFERENCES

- Abeles, F.B. (1968). The role of RNA and protein synthesis in abscission. *Plant Physiol.* **43**, 1577-1586.
- Addicott, F.T. (1982). *Abscission*. (Berkeley: University of California Press).
- Baumbusch, L.O., Thorstensen, T., Krauss, V., Fischer, A., Naumann, K., Assalkhou, R., Schulz, I., Reuter, G., and Aalen, R.B. (2001). The *Arabidopsis thaliana* genome contains at least 29 active genes encoding SET domain proteins that can be assigned to four evolutionarily conserved classes. *Nucleic Acids Res.* **29**, 4319-4333.
- Bleecker, A., and Patterson, S.E. (1997). Last exit: Senescence, abscission, and meristem arrest in Arabidopsis. *Plant Cell* **9**, 1169-1179.

- Bleecker, A.B., Estelle, M.A., Somerville, C., and Kende, H. (1988). Insensitivity to ethylene conferred by a dominant mutation in *Arabidopsis thaliana*. *Science* **241**, 1086–1089.
- Bowman, J. (1994). *Arabidopsis: An Atlas of Morphology and Development*. (New York: Springer-Verlag).
- Brown, K.M. (1997). Ethylene and abscission. *Physiol. Plant.* **100**, 567–576.
- Chen, Q.G., and Bleecker, A.B. (1995). Analysis of ethylene signal-transduction kinetics associated with seedling-growth response and chitinase induction in wild-type and mutant *Arabidopsis*. *Plant Physiol.* **108**, 597–607.
- Clough, S.J., and Bent, A.F. (1998). Floral dip: A simplified method for *Agrobacterium*-mediated transformation of *Arabidopsis thaliana*. *Plant J.* **16**, 735–743.
- Cock, J.M., and McCormick, S. (2001). A large family of genes that share homology with CLAVATA3. *Plant Physiol.* **126**, 939–942.
- Fernandez, D.E., Heck, G.R., Perry, S.E., Patterson, S.E., Bleecker, A.B., and Fang, S.C. (2000). The embryo MADS domain factor AGL15 acts postembryonically: Inhibition of perianth senescence and abscission via constitutive expression. *Plant Cell* **12**, 183–198.
- Fletcher, J.C., Brand, U., Running, M.P., Simon, R., and Meyerowitz, E.M. (1999). Signaling of cell fate decisions by CLAVATA3 in *Arabidopsis* shoot meristems. *Science* **283**, 1911–1914.
- Gomez-Gomez, L., and Boller, T. (2000). FLS2: An LRR receptor-like kinase involved in the perception of the bacterial elicitor flagellin in *Arabidopsis*. *Mol. Cell* **5**, 1003–1011.
- González-Carranza, Z.H., Loyola-Gloria, E., and Roberts, J.A. (1998). Recent developments in abscission: Shedding light on the shedding process. *Trends Plant Sci.* **3**, 10–14.
- González-Carranza, Z.H., Whitelaw, C.A., Swarup, R., and Roberts, J.A. (2002). Temporal and spatial expression of a polygalacturonase during leaf and flower abscission in oilseed rape and *Arabidopsis*. *Plant Physiol.* **128**, 534–543.
- Grbic, V., and Bleecker, A.B. (1995). Ethylene regulates the timing of leaf senescence in *Arabidopsis*. *Plant J.* **8**, 595–602.
- Grini, P.E., Jurgens, G., and Hulskamp, M. (2002). Embryo and endosperm development is disrupted in the female gametophytic capulet mutants of *Arabidopsis*. *Genetics* **162**, 1911–1925.
- Guzman, P., and Ecker, J.R. (1990). Exploiting the triple response of *Arabidopsis* to identify ethylene-related mutants. *Plant Cell* **2**, 513–523.
- Hajdukiewicz, P., Svab, Z., and Maliga, P. (1994). The small, versatile pPZP family of *Agrobacterium* binary vectors for plant transformation. *Plant Mol. Biol.* **25**, 989–994.
- Jinn, T.L., Stone, J.M., and Walker, J.C. (2000). HAESA, an *Arabidopsis* leucine-rich repeat receptor kinase, controls floral organ abscission. *Genes Dev.* **14**, 108–117.
- Kieber, J.J., Rothenberg, M., Roman, G., Feldmann, K.A., and Ecker, J.R. (1993). CTR1, a negative regulator of the ethylene response pathway in *Arabidopsis*, encodes a member of the Raf family of protein kinases. *Cell* **72**, 427–441.
- Lanahan, M.B., Yen, H.-C., Giovannoni, J.J., and Klee, H. (1994). The never ripe mutation blocks ethylene perception in tomato. *Plant Cell* **6**, 521–530.
- Li, J., and Chory, J. (1997). A putative leucine-rich repeat receptor kinase involved in brassinosteroid signal transduction. *Cell* **90**, 929–938.
- Mandal, A., Sandgren, M., Holmstrom, K.-O., Gallois, P., and Palva, E.T. (1995). Identification of *Arabidopsis thaliana* sequences responsive to low temperature and abscisic acid by T-DNA tagging and *in vivo* gene fusion. *Plant Mol. Biol. Rep.* **13**, 243–254.
- Mao, L., Begum, D., Chuang, H.W., Budiman, M.A., Szymkowiak, E.J., Irish, E.E., and Wing, R.A. (2000). *JOINTLESS* is a MADS-box gene controlling tomato flower abscission zone development. *Nature* **406**, 910–913.
- Meza, T.J., Stangeland, B., Mercy, I.S., Skårn, M., Nymoen, D.A., Berg, A., Butenko, M.A., Håkelién, A.-M., Haslekås, C., Meza-Zepeda, L.A., and Aalen, R.B. (2002). Analyses of single-copy *Arabidopsis* T-DNA transformed lines show that the presence of vector backbone sequences, short inverted repeats and DNA methylation is not sufficient or necessary for the induction of transgene silencing. *Nucleic Acids Res.* **30**, 4556–4566.
- Murashige, T., and Skoog, F. (1962). A revised medium for rapid growth and bioassays with tobacco tissue culture. *Physiol. Plant.* **15**, 473–497.
- Nielsen, H., Engelbrecht, J., Brunak, S., and von Heijne, G. (1997). Identification of prokaryotic and eukaryotic signal peptides and prediction of their cleavage sites. *Protein Eng.* **10**, 1–6.
- Patterson, S.E. (2001). Cutting loose: Abscission and dehiscence in *Arabidopsis*. *Plant Physiol.* **126**, 494–500.
- Patterson, S.E., Huelster, S.M., and Bleecker, A. (1994). Floral organ abscission in *Arabidopsis thaliana*. *Plant Physiol.* **105**, 181 (abstr.).
- Payton, S., Fray, R.G., Brown, S., and Grierson, D. (1996). Ethylene expression is regulated during fruit ripening, flower senescence and abscission. *Plant Mol. Biol.* **31**, 1227–1231.
- Roberts, J.A., Schindler, C.B., and Tucker, G.A. (1984). Ethylene-promoted tomato flower abscission and the possible involvement of an inhibitor. *Planta* **160**, 159–163.
- Rojo, E., Sharma, V.K., Kovaleva, V., Raikhel, N.V., and Fletcher, J.C. (2002). CLV3 is localized to the extracellular space, where it activates the *Arabidopsis* CLAVATA stem cell signaling pathway. *Plant Cell* **14**, 969–977.
- Roman, G., Lubarsky, B., Kieber, J.J., Rothenberg, M., and Ecker, J.R. (1995). Genetic analysis of ethylene signal transduction in *Arabidopsis thaliana*: Five novel mutant loci integrated into a stress response pathway. *Genetics* **139**, 1393–1409.
- Sexton, R., Lewis, L.N., Trewavas, A.J., and Kelly, P. (1985). Ethylene and abscission. In *Ethylene and Plant Development*, J.A. Roberts and G.A. Tucker, eds (London: Butterworths), pp. 173–196.
- Sexton, R., and Roberts, J.A. (1982). Cell biology of abscission. *Annu. Rev. Plant Physiol.* **33**, 133–162.
- Sharma, V.K., Ramirez, J., and Fletcher, J.C. (2003). The *Arabidopsis* *CLV3-like* (*CLE*) genes are expressed in diverse tissues and encode secreted proteins. *Plant Mol. Biol.* **51**, 415–425.
- Shiu, S.H., and Bleecker, A.B. (2001). Plant receptor-like kinase gene family: Diversity, function, and signaling. *Sci. STKE* **2001**, RE22.
- Van Doorn, W.G., and Stead, A.D. (1997). Abscission of flowers and floral parts. *J. Exp. Bot.* **48**, 821–837.
- Vanoosthuyse, V., Miegé, C., Dumas, C., and Cock, J.M. (2001). Two large *Arabidopsis thaliana* gene families are homologous to the *Brassica* gene superfamily that encodes pollen coat proteins and the male component of the self-incompatibility response. *Plant Mol. Biol.* **46**, 17–34.
- von Arnim, A.G., Deng, X.W., and Stacey, M.G. (1998). Cloning vectors for the expression of green fluorescent protein fusion proteins in transgenic plants. *Gene* **221**, 35–43.
- Wilkinson, J.Q., Lanahan, M.B., Clark, D.G., Bleecker, A.B., Chang, C., Meyerowitz, E.M., and Klee, H.J. (1997). A dominant mutant receptor from *Arabidopsis* confers ethylene insensitivity in heterologous plants. *Nat. Biotechnol.* **15**, 444–447.
- Woltering, E.J., and Van Doorn, W.G. (1988). Role of ethylene in senescence of petals: Morphological and taxonomical relationships. *J. Exp. Bot.* **39**, 1605–1616.